ELSEVIER

Contents lists available at ScienceDirect

### **Materials Letters**

journal homepage: www.elsevier.com/locate/matlet



# Enhanced adsorption and photocatalysis properties of molybdenum oxide ultrathin nanobelts



Y.F. Zhou<sup>a</sup>, K. Bi<sup>a</sup>, L. Wan<sup>a</sup>, X. Ji<sup>a</sup>, C. Wen<sup>a</sup>, K. Huang<sup>a</sup>, C. Liang<sup>a</sup>, Z.B. Sun<sup>b,\*</sup>, D.Y. Fan<sup>a</sup>, H.J. Yang<sup>a</sup>, Y.G. Wang<sup>a</sup>, M. Lei<sup>a,\*</sup>

#### ARTICLE INFO

Article history: Received 22 February 2015 Accepted 16 April 2015 Available online 24 April 2015

Keywords: Semiconductors Nanocrystalline materials Microstructure

#### ABSTRACT

The alpha molybdenum oxide  $(\alpha\text{-MoO}_3)$  ultrathin nanobelts are prepared by a two-step hydrothermal method. The original MoO<sub>3</sub> nanobelts are first prepared using molybdenyl acetylacetonate as a single precursor, and then followed by reprocessing with hydrogen peroxide  $(H_2O_2, 30\%)$ . The characterization results indicate that the products grow with the preferred orientation of [001] and become much thinner after reprocessing with  $H_2O_2$ . The formation process is ascribed to that peroxide species sterically break the framework of  $MoO_6$  octahedra sheets, resulting in the ultrathin formation of  $MoO_3$ . Moreover, the adsorption and photocatalysis of the  $MoO_3$  ultrathin nanobelts indicate that the adsorption rate of the  $MoO_3$  nanobelts increases from 6.98% to 30.02% and photocatalytic degradation rate promotes from 52.03% to 79.55%, respectively.

© 2015 Elsevier B.V. All rights reserved.

#### 1. Introduction

Because of their fundamental interest, as well as potential applications in nanostructure-based photonics and electronics, considerable attention has been focused on the syntheses and properties of semiconductor nanostructures [1-10]. Among these nanostructures, alpha molybdenum oxide (α-MoO<sub>3</sub>) with thermodynamical stability and unique double-layered structure has attracted considerable attention due to its potential applications such as sensor, photocatalyst, supercapacitor, and battery electrodes [11–14]. As is well known, the morphology and size of semiconductors have strong influence on the related physical and chemical properties. Therefore, considerable effort has focused on the synthesis of various  $\alpha$ -MoO<sub>3</sub> nanostructures. To date, various morphologies of α-MoO<sub>3</sub>, such as nanobelts, nanowires, nanorods, and nanotubes, have been successfully prepared by various routes including laser deposition, electrodeposition, CVD, hydrothermal route etc. [15–18]. Additionally, the pollution, high-cost, low output and other problems of the preparations hinder the development of nanomaterials; thus the low-cost, only the water as its byproducts and no pollutions for the environment decide that the hydrogen peroxide is widely employed to prepare various nanomaterials such as CdO, TiO<sub>2</sub>,  $V_2O_5$  and so on [19–21]. Herein,  $\alpha$ -MoO<sub>3</sub>

E-mail addresses: zbsunnssc@sohu.com (Z.B. Sun), minglei@bupt.edu.cn (M. Lei).

ultrathin nanobelts are prepared by a two-step hydrothermal method. The original MoO $_3$  nanobelts are first prepared using molybdenyl acetylacetonate as a single precursor, and then followed by reprocessing with 30% H $_2$ O $_2$ . It is found that the nanobelts turned much thinner after being treated with H $_2$ O $_2$ . Moreover, the waste water treatment test showed that the adsorption and photocatalysis efficiency of  $\alpha$ -MoO $_3$  nanobelts for wastewater greatly increased when the nanobelts grew much thinner.

## 2. Experimental

In a typical synthesis, 0.625 g molybdenyl acetylacetonate was added into the solution with 7.855 ml of nitric acid and 27.145 ml of distilled water in a beaker. After stirring for 1 h, the solution was transferred into a 50 ml of Teflon-sealed autoclave and maintained at 180 °C for 48 h. When cooling down to the room temperature, the resultant product was obtained, washed with the DI water and ethanol several times and dried at 60 °C overnight. Subsequently, 82 mg of powder obtained by the above section was added into the solution with 8.5 ml of distilled water and 8.5 ml of 30%  $H_2O_2$  in a beaker. After stirring for 11 h in the dark, the color of the solution changed from white to yellow, the solution was transferred into a 50 ml of Teflon-sealed autoclave and maintained at 170 °C for 24 h. Cooling down to the room temperature, washed with the DI water and ethanol several times and dried at 60 °C overnight, the ultrathin  $\alpha$ -MoO3 nanobelts were obtained and then were characterized by

<sup>&</sup>lt;sup>a</sup> State Key Laboratory of Information Photonics and Optical Communications & School of Science, Beijing University of Posts and Telecommunications, Beijing 100876, China

b Center for Space Science and Applied Research, National Space Science Center, Chinese Academy of Sciences, Beijing 100190, China

<sup>\*</sup> Corresponding authors.

XRD, Raman spectra, SEM, TEM and BET. The absorptivity and photocatalysis of the samples were evaluated through the decomposition of methyleneblue (MB) dye at ambient temperature according to the literature [22]. The concentration change of dye was monitored with a UV–vis spectrophotometer (SPECORD 200) at a given time interval.

#### 3. Results and discussion

To understand the structure, the preferred orientation of the growth of the samples and the change when the nanobelts are treated with H<sub>2</sub>O<sub>2</sub>, the samples are first characterized by the XRD and Raman spectra as shown in the Fig. 1A and B, separately. We can see that the main diffraction peaks appears at 12.8°, 25.7° and 39.0°, which well agrees with the (020), (040) and (060) planes of an orthorhombic phase of MoO<sub>3</sub> (JCPDS 35-0609), respectively. Additionally, the XRD patterns are sharp and no other peaks exist, therefore the samples are well crystallized and have no other impurities. The Fig. 1A shows that the strongest diffraction peak appears at the (040) plane, thence the [001] is the preferred orientation of the crystal growth [26]. After being reprocessed with H<sub>2</sub>O<sub>2</sub>, the FWHM of diffraction peaks broaden from 0.18°,  $0.17^{\circ}$  and  $0.21^{\circ}$  to  $0.25^{\circ}$ ,  $0.24^{\circ}$  and  $0.28^{\circ}$ at the planes of (020), (040) and (060), respectively, which indicates that the grain sizes become smaller depending on the Scherrer formula. In order to further determine the structures and the change of the samples after being reprocessed with H<sub>2</sub>O<sub>2</sub>, the Raman spectra are carried out as shown in the Fig. 1B. The three main peaks, located in 661.4, 821.32 and 995.96 cm<sup>-1</sup>, are consistent with the vibration modes of  $\alpha$ -MoO<sub>3</sub>. The peak of terminal oxygen (Mo = 0) stretching mode appears at 995.96 cm<sup>-1</sup>, the doubly coordinated bridging oxygen  $(Mo_2-0)$  stretching mode's peak is at 821.32 cm<sup>-1</sup> and the peak at 663.24 cm<sup>-1</sup> is the triply coordinated oxygen (Mo<sub>3</sub>-O) stretching mode [11]. In addition, when the MoO<sub>3</sub> nanobelts are reprocessed with H<sub>2</sub>O<sub>2</sub>, the width of the spectra peaks broaden from 13.57, 21.73 and 8.91 cm<sup>-1</sup> to 15.04, 23.09 and 9.213 cm<sup>-1</sup> at the peak of 663.24, 821.32 and 994.12 cm<sup>-1</sup>, moreover the peak at 994.12 cm<sup>-1</sup> shifted to 995.96 cm<sup>-1</sup>, which further indicates that the grain sizes become smaller. Therefore, the Raman spectra further confirm that the grain sizes of MoO<sub>3</sub> become smaller after being reprocessed with H<sub>2</sub>O<sub>2</sub>, well consistent with the analysis of the

The fresh  $MoO_3$  nanobelts and  $MoO_3$  reprocessed with  $H_2O_2$  were further characterized by SEM and TEM image. As shown

in the Fig. 2A and B, we find that the both samples consist of nanobelts with uniform size. Comparing the Fig. 2A with B, it is found that, when the samples are reprocessed with  $H_2O_2$ , the aspect ratios of the nanobelts are larger, the edges change smoother and the nanobelts become much thinner. Additionally, the Fig. 2C and D are the TEM images of the MoO<sub>3</sub> reprocessed with  $H_2O_2$ , the Fig. 2C further evidences the belt-like shape of the products and the selected area electron diffraction (SAED) pattern implies that the samples have a single crystal structure, the length and width of the nanobelts are along with the crystal orientation of [001] and [100], respectively. The HRTEM image (Fig. 2D) shows that the space between two lattice fringes is 0.37 nm, corresponding to the plane of (001) and indicating the preferential growth along the [001], which is consistent with the analysis of the XRD.

It can be concluded that, when the  $MoO_3$  nanobelts are reprocessed with  $H_2O_2$ , the nanobelts turn much thinner. As shown in the Fig. 3, the  $MoO_3$  nanobelts consist of  $MoO_6$  octahedra sheets, when the  $H_2O_2$  is added into the beaker containing  $MoO_3$  nanobelts, some  $MoO_6$  octahedra sheets begin to react with  $H_2O_2$  and form the molybdenum peroxide. However, the molybdenum peroxide is unstable, during thermal treatment the molybdenum peroxide will decompose. In the process, peroxide species sterically hinder the formation of the oxide framework, which will break some  $MoO_6$  octahedra sheets and make the  $MoO_3$  nanobelts become thinner [23]. Moreover, the stick force between two  $MoO_6$  octahedra sheets is lower than that in the same sheet, which also somehow promotes the formation and thinning nanobelts [23].

The adsorption and photocatalysis of the nanomaterials are structure-sensitive to understand the effects of the morphologies on them, we study the impacts for wastewater treatment of MoO<sub>3</sub> nanobelts when they are reprocessed with H<sub>2</sub>O<sub>2</sub> by the degradation of MB as the model reaction [24]. The result is as shown in the Fig. 4A, the wastewater treatment experiment consists of two successive parts, the adsorption and photocatalytic degradation. To ensure the completion of the adsorption, the photocatalytic degradation is carried on after adsorption 60 min. The Fig. 4A shows that when the samples are reprocessed with H<sub>2</sub>O<sub>2</sub>, the adsorption rate of the MoO<sub>3</sub> nanobelts increase from 6.98% to 30.02%. The reason is that after being reprocessed with H<sub>2</sub>O<sub>2</sub>, the nanobelts turn thinner, which makes the specific surface area of nanobelts larger and increase the adsorption rate. Additionally, H<sub>2</sub>O<sub>2</sub> promotes the photocatalytic degradation rate of MoO<sub>3</sub> nanobelts from 52.03% to 79.55%. To better analyze the reasons for the improvement of the photocatalytic degradation rate, we measure the specific surface area (BET) of the nanobelts by the

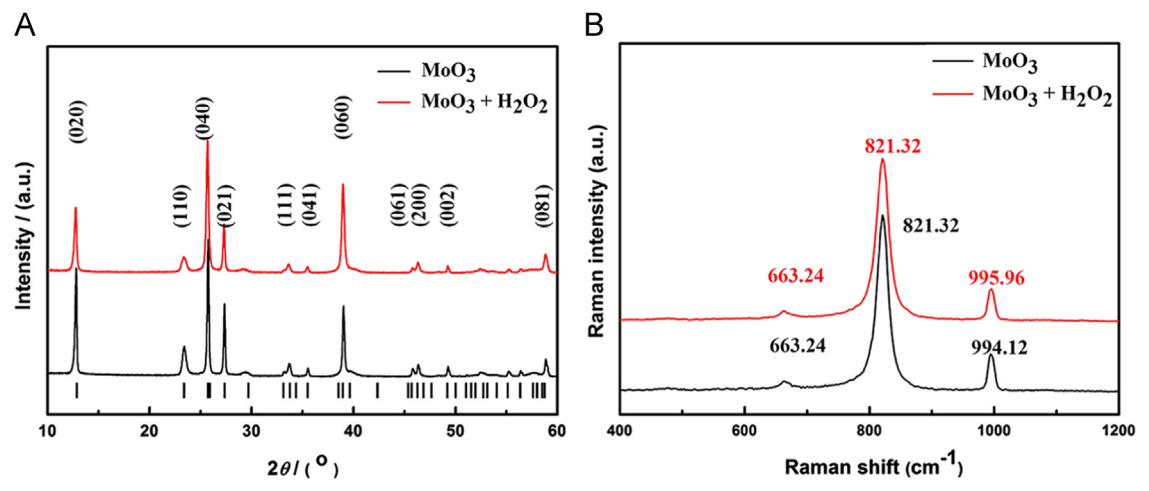


Fig. 1. (A) XRD pattern and (B) Raman pattern of the synthesized MoO<sub>3</sub> and the reprocessed MoO<sub>3</sub> with H<sub>2</sub>O<sub>2</sub>.

# Download English Version:

# https://daneshyari.com/en/article/1642616

Download Persian Version:

https://daneshyari.com/article/1642616

<u>Daneshyari.com</u>